Int. J. Heat Mass Transfer. Vol. 34, No. 2, pp. 427–435, 1991
Printed in Great Britain

0017–9310/91 $3.00 + 0.00

Wall-to-bed contact heat transfer rates in mechanically stirred granular beds

KARUN MALHOTRA† and ARUN S. MUJUMDAR
Department of Chemical Engineering, McGill University, Montreal, Canada

(*Received* 22 *August* 1989 *and in final form* 26 *March* 1990)

Abstract—This paper presents experimental and simulated results for the wall-to-bed contact heat transfer coefficient in granular beds stirred by paddle-type blades. The experimental observations are shown to be predicted fairly well by the particle renewal model for contact heat transfer. The effects of agitator speed, wall-to-blade clearance, solids flowability, air flow rate and particle surface roughness on contact heat transfer rates are presented and discussed.

INTRODUCTION

INDIRECTLY heated agitated vessels are widely used as dryers, heat exchangers, calciners and have possible applications as polymerization reactors, adsorbers, etc. An industrial paddle-type stirred vessel is typically a long horizontal trough with flat rectangular cross-sectioned blades mounted along the central agitator shaft. In case of indirect heating, heat is supplied through the walls and sometimes through the hollow agitator shaft and the blades. Such equipment has been illustrated by Root [1], Ohashi [2] and McCormick [3] and finds wide ranging applications in industries processing products such as minerals and ores, chemicals, pharmaceuticals, polymers and food.

The merits and demerits of such equipment and in general indirectly heated agitated vessels are outlined in several references (e.g. see refs. [4–6]). In separate publications [5, 6] the authors have discussed the development of a contact heat transfer model based on the particle renewal rates at the heated surface in granular beds stirred by paddle-type blades. This paper presents and discusses the theoretically simulated and experimental results of the wall-to-bed contact heat transfer coefficient. The experimental observations include the effects of agitator rotational speed (N), size of the wall-to-blade clearance (δ), solids flowability (C), air flow rate (U) and particle surface roughness (s_r).

EXPERIMENTAL APPARATUS AND PROCEDURE

The experimental set-up consisted of a vessel stirred by paddle-type blades and driven via a flexible coupling connecting the agitator shaft to a drive consisting of two belt-driven pulleys and a variable speed d.c. motor. The heat transfer vessel was 0.25 m in diameter and 0.15 m in depth (axially). It consisted of a perforated grid with an open area of 16% (1.6 mm holes on a 3.8 mm triangular pitch) and circumferential length 0.125 m. The vessel is illustrated in Fig. 1. The plenum chamber was filled with spherical glass beads to dampen turbulence in the air flow.

The vessel was heated through the side walls by four heater assemblies, two on each side of the grid (H1 through H4 in Fig. 1). A heater assembly consisted of a 3 mm thick copper plate (one surface contacting the granular bed) bonded on the back (with a fine layer of silicone rubber epoxy) to a flexible, uniform heat flux, etched foil silicone heater (Sakaguchi Electrical Heaters, Tokyo, Japan). A second flexible heater acting as a guard against radial heat losses, was bonded on the back of the first one with a 2 mm thick insulating sheet in between. The heater bonded to the copper plate supplied heat to the system. The heater assemblies were insulated from the vessel and each other by low thermal conductivity rubber O-rings.

The temperature difference between the guard and the main heater was maintained within 2°C (the guard heater always maintained at lower temperature) by a proportional temperature controller to reduce radial heat losses. The sides of the vessel were also insulated with 30 mm thick glass wool sheets. The heat losses even with the guard heaters switched off were estimated to be less than 3%.

The heat input to all the four heaters could be individually monitored and switched on or off. The power input to all the heaters varied within ±6%. The surface temperatures were monitored on a digital thermometer via constantan–copper thermocouples (nominal size 0.56 mm) fused 1 mm below the surface of the copper plates (in contact with the bed) with a highly conducting silver emulsion epoxy. The thermocouples were positioned centrally at eight different locations along the side walls, two on each heated surface, 30 mm from the ends as shown in Fig. 1.

The size of the wall-to-blade clearance was varied between 2.3 and 37 mm. The wall-to-blade clearance region in this study is defined as the annular zone in

† Present address: Murata Manufacturing Co. Ltd, Nagaoka-Shi, Kyoto 617, Japan.

NOMENCLATURE

B	blade height [m]
C	modified bulk compressibility of solids [—]
C_b	specific heat of granular bed [J kg^{-1} K^{-1}]
D	vessel diameter [m]
d_p	characteristic particle dimension [mm]
$E(t)$	expected value of particle–surface contact time (equation (16)) [—]
F	fraction of vessel circumferential area covered with particles [—]
H	average bed height at central midplane [m]
h	local wall-to-bed contact heat transfer coefficient [W m^{-2} K^{-1}]
h_{av}	overall wall-to-bed contact heat transfer coefficient [W m^{-2} K^{-1}]
k_f	fluid thermal conductivity [W m^{-1} K^{-1}]
L	circumferential length of particle covered surface area [m]
l	linear separation between two adjacent b1 blades [m]
N	agitator rotational speed [rev min^{-1}]
N_b	number of blade passes (b1) required for a particle along the wall to traverse the distance L [—]
Nu	local Nusselt number, $hd_pk_f^{-1}$ [—]
Nu_{av}	average Nusselt number, $h_{av}d_pk_f^{-1}$ [—]
n	number of b1 blades mounted on the shaft in the same axial and radial planes [—]
s_r	average size of surface asperities on contacting surfaces [m]
t	particle–surface contact time [s]
t_{av}	average particle–surface contact time [s]
Δt	time taken per pass of blade b1 [s]
ΔT	average wall-to-bed temperature gradient [K]
U	superficial air velocity through the bed [m s^{-1}]
U_{mf}	minimum fluidization velocity [m s^{-1}]
x	instantaneous particle position along the wall [m]
Δx	average particle displacement per blade pass along the wall [m].

Greek symbols

δ	thickness of the wall-to-blade clearance region [mm]
ε	average porosity of the granular bed [—]
η_0	efficiency of particle renewal [—]
Π	region of influence of the moving blade [m]
ρ_b	bulk density of the granular bed [kg m^{-3}].

the bed between the cylindrical vessel wall and the surface swept by the outer tip of the rotating blade. The experimental uncertainty in evaluation of the average wall-to-bed heat transfer coefficient (h_{av}) was estimated at $\pm 11\%$. The heat transfer measurements were reproducible within $\pm 6\%$. The heat transfer coefficients were also found to be independent of the heat flux (50–200% range) over the entire range of operating parameters.

The range of the operating parameters and the thermophysical properties of the granular bed and particles are available in the companion paper [5].

The heat transfer experiments were performed under 'quasi-steady state' conditions. A known weight of the solids at room temperature (20–25°C) was loaded in the vessel and the air flow set to the desired level. The heat input was then adjusted to obtain the desired range of wall temperatures. 'Steady state' was assumed when the variation in the wall temperatures was typically less than 0.1°C over 4 min. After recording the wall, inlet and outlet air temperatures, the air and heat supply were shut off simultaneously. The bed temperature (T_b) was then measured immediately thereafter at different radial locations by inserting a thermocouple from the hood.

DATA ANALYSIS

The bed temperatures were recorded at two radial locations—10–$15d_p$ deep from the bed surface and 2–3 cm above the longer blade (b1 in Fig. 1). Temperature variations as high as 2–3°C (as compared to $\Delta T = 5$–15°C) were observed under most operating conditions. However for $N > 10$ rev min^{-1} and $U/U_{mf} \geqslant 0.4$, the bed was thermally well mixed (temperature variation ± 0.3°C). The inlet and outlet air temperatures were also recorded.

The local wall-to-bed heat transfer coefficients (h) were defined as

$$h = Q/\Delta T \tag{1}$$

where Q is the local heat flux and ΔT the local wall-to-bed temperature difference at a given thermocouple location. The local Nusselt number (Nu) was then determined as

$$Nu = hd_p/k_f. \tag{2}$$

The average Nusselt number, Nu_{av}, was defined as

$$Nu_{av} = h_{av}d_p/k_f \tag{3}$$

where h_{av} is the average heat transfer coefficient. Note, that h_{av} is evaluated as the average of local values of

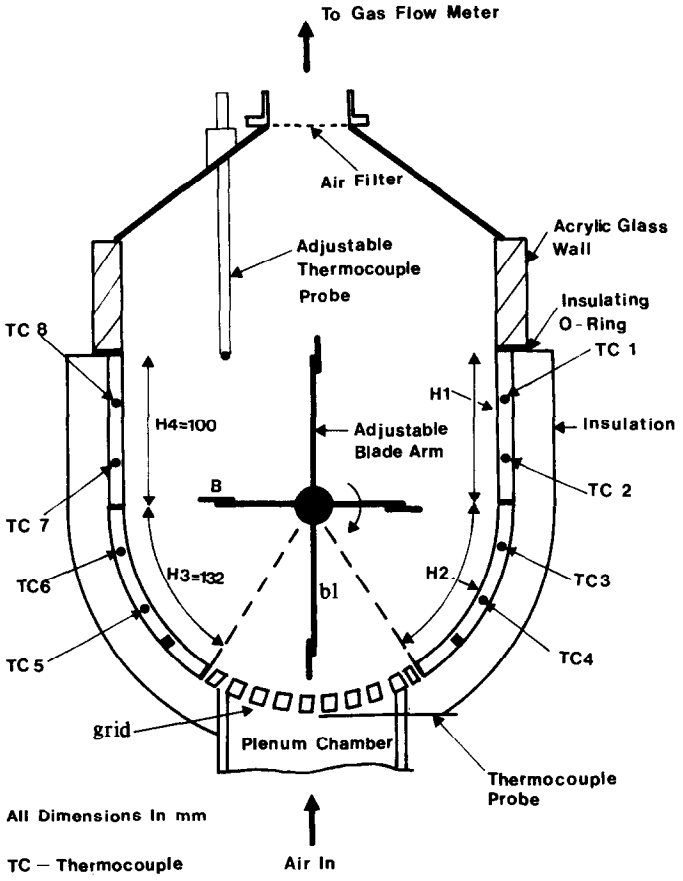

FIG. 1. Front view of the heat transfer apparatus.

h for heaters in operation. For example, for $H/B \leqslant 5$, heater H1 was almost bare and was therefore switched off. In this case h_{av} refers to the average values of h for heaters H2 through H4.

Evaluation of the representative bed temperature to be used in the definition of ΔT poses a major problem in such vessels. For packed granular beds flowing over a heated plate most authors [7–9] measured the bed temperature of the solids upstream of the heated surface. Other researchers [10, 11] do not explicitly mention the procedure for determining the bed temperature in stirred granular beds. However, they assume the bed to be thermally well mixed.

As discussed by the authors in separate publications [4, 12, 13] the bulk of the granular bed does not get randomly mixed after every blade pass. Uniform bulk solids mixing is achieved after a certain number of blade passes. The existence of thermal gradients within a granular bed is a function of the particle trajectories (and thermal history) and the rate of particle renewal at the heated surface. For example, a 'heated' particle in the bed may not have sufficient time to achieve thermal equilibrium with the rest of the bulk, before contacting the heated surface again. This leads to 'short-circuiting' of heated particles. Similarly, some particles may not contact the heat transfer surface at all during operation [12–14]. Therefore, thermal gradients are expected to be present within the granular bed.

Particle renewal has been shown [4, 13] to occur behind the moving blade from the bulk. Therefore, the temperature of the 'freshly renewed packet' of particles is most likely to be equal to the bed temperature at the location where such renewal is occurring. Particle renewal along heaters 2 and 4 was observed to occur mainly from the particle layers near the bed surface. Therefore, the average temperature recorded by thermocouples $10–15d_p$ from the bed surface was chosen as the bed temperature corresponding to heaters H2 and H4. For heater H3, the average temperature of solids 2–3 cm above blade bl (when blade bl is over H3) was selected as the bed temperature in the computation of h.

RESULTS AND DISCUSSIONS

Background

The following expression for estimating particle renewal efficiency (η_0) along the vessel wall in the wall-to-blade clearance region was proposed in refs. [4, 6]:

$$\eta_0 = 1-\exp\left\{-\eta_0\left[1+\left(1+\frac{\Delta x}{\Pi}\right)\frac{\eta_0}{2}\right]\right\}. \quad (4)$$

The above equation was derived assuming a parabolic particle velocity profile along the wall upstream of the moving blade. The extent of the zone where particle movement occurs is denoted by Π and is defined [4, 6] as the upstream region of influence (along the wall) exerted by the moving blade. The average particle displacement per blade pass at a given location along the vessel cylindrical wall is denoted by Δx. Except for particles with reduced flowability [4, 13], $\Delta x/L < 1$. Generally, $\Delta x/L$ increases almost linearly with x [4, 6]. The particle position at any given location along the wall is denoted by x, with its origin at the point of blade entry into the granular bed.

The solids flowability has been characterized by the 'modified bulk compressibility' (C) [4, 13] in terms of the difference in the bulk densities of the granular bed in packed and normal states. In beds stirred by paddle-type blades, particles with $C \leqslant 0.08$ are labelled as free-flowing, while solids with $C \geqslant 0.11$ exhibit reduced flowability. Granular beds with $C \geqslant 0.11$ flow as a 'plug' upstream of the blade under certain operating conditions [4, 6, 12, 13].

The particle renewal efficiency is a function of the particle position, because Δx and Π both vary with x [4, 6]. However, an expression was developed in ref. [5] for the average particle–surface contact time (t_{av}) based on a simplified model assuming Δx and η_0 to be constant along the heated surface area of the granular bed (i.e. for $0 \leqslant x \leqslant L$). This assumption does not introduce significant errors in estimating t_{av}, because the ratio $\Delta x/\Pi$ does not vary much with x [4, 6]. The final expression for t_{av}, derived from the binomial probability distribution is given as

$$t_{av} = E(t)\cdot\Delta t \quad (5)$$

where

$$E(t) = \sum_{j=0}^{N_b-1}\frac{N_b!}{j!(N_b-j)!}\eta_0^{N_b-j}(1-\eta_0)^j(j+1) + N_b(1-\eta_0)^{N_b} \quad (6)$$

and

$$N_b = \frac{L}{\Delta x}.$$

The time interval between two successive blade passes is given by Δt, while the 'expectation value' of contact time is denoted by $E(t)$. Equation (5) may be used in conjunction with existing theories on particle–surface contact heat transfer (e.g. refs. [5, 7, 9]) to evaluate the wall-to-bed average heat transfer coefficient (h_{av}).

For particles exhibiting 'plug flow' under certain operating conditions (rice and linseed; $\delta/d_p \leqslant 5$ for $D = 0.5$ m and $\delta/d_p \leqslant 3$ for $D = 0.25$ m), h_{av} may be evaluated by the following equations [4, 5]:

$$h_{av} = \frac{l}{2L\Delta t}\int_{t_R-\Delta t}^{t_R+\Delta t} h\,dt \quad n > \frac{\pi D}{L} \quad (7)$$

$$t_R = \frac{N\cdot L}{\pi D\cdot 60}$$

$$h_{av} = \frac{1}{2t_R}\int_{\Delta t-t_R}^{\Delta t+t_R} h\,dt \quad n \leqslant \frac{\pi D}{L}. \quad (8)$$

Equation (7) takes into account the reduction in the particle renewal area when more than one blade is immersed in the bed at any instant. The time a given blade remains immersed within the bed is denoted by t_R. The local wall-to-bed contact heat transfer coefficient (h) may be evaluated from expressions proposed in refs. [4, 5, 15].

Simulated results

In industrial practice, indirect heat is supplied mainly via the latent heat of a condensing gas medium. Therefore, the theoretical simulations presented in this paper assume an isothermal heat transfer surface area. Figure 2 presents the simulation results obtained from equation (8) for a bed of rice particles. It is clear that while increasing N enhances the heat transfer rate, this increase is significant mainly at lower rotational speeds, i.e. $N \leqslant 15$ rev min^{-1}. Whereas a six-fold increase in N from 2.5 to 15 rev min^{-1} enhances Nu_{av} by about 60% for $d_p = 1.7$ mm, the corresponding increase is about 35% for N increased from 15 to 90 rev min^{-1}. This is consistent with the experimental results presented later.

Also, Nu_{av} increases with increasing d_p. This follows from the fact that for fine particles ($d_p < 1$ mm) the overall heat transfer coefficient is controlled by the resistance to heat conduction in the packed bed over the entire range of particle–surface contact times encountered in this study [4, 5]. Heat conduction in packed beds is a function of the bed physio-thermal properties and particle–surface contact time, but independent of particle size. However, the wall-to-first particle layer thermal contact resistance (in series with the conduction resistance) is a function of fluid

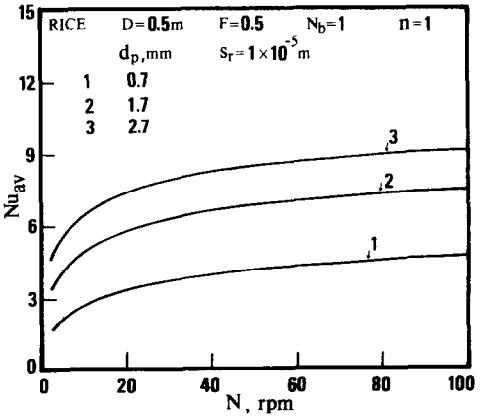

FIG. 2. Effect of d_p on Nu_{av} for $N_b = 1$.

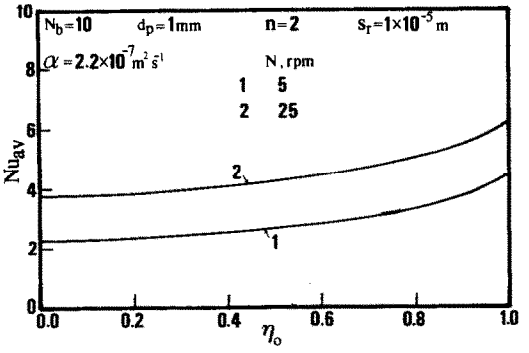

FIG. 3. Effect of η_0 on Nu_{av}.

properties, bed porosity and d_p only, and varies inversely with the particle diameter. Therefore, for fine particles, resistance due to heat conduction in the packed bed controls h. Heat conduction resistance is also the controlling factor for contact times when the thermal penetration is well beyond several particle layers. The above-mentioned reasons lead to lower values of Nu_{av} for finer particles (although h_{av} is higher than coarser ones).

The above results imply that mechanically stirred vessels may not be suitable for very fine particles with respect to maximizing h_{av}. Equipment such as vibrated and conventional fluidized beds [16] allowing very short particle–surface contact times to be achieved are probably better suited for finer particles. Similar conclusions may be drawn for beds of free-flowing glass or millet particles.

For cases where there is particle renewal along the wall ($N_b > 1$), two parameters, N_b and η_0, are required to estimate h_{av}. The effects of these parameters are displayed in Figs. 3 and 4. Figure 3 shows that increasing η_0 enhances Nu_{av} for a given value of N_b. The increase in Nu_{av} is most significant beyond $\eta_0 > 0.7$. The upper and lower bounds for Nu_{av} correspond to $\eta_0 = 1$ and 0 (equations (4) and (5)), respectively. The difference between the two extrema is almost 100% for $N = 5$ rev min^{-1} and 65% for $N = 25$ rev min^{-1}. This implies that for a constant

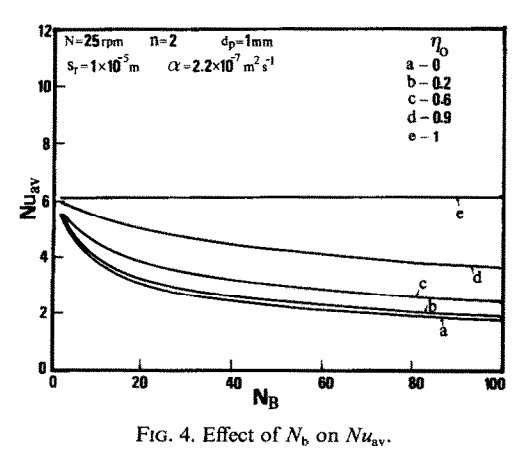

FIG. 4. Effect of N_b on Nu_{av}.

N_b, the adverse effect of decreasing η_0 on Nu_{av} diminishes with increasing N.

Figure 4 presents a family of Nu_{av} curves for $N = 25$ rev min^{-1} with η_0 as a parameter. For $\eta_0 = 1$, Nu_{av} is independent of N_b and is a function of N only. There is a sharp reduction in Nu_{av} with increasing N_b for $N_b \leqslant 10$. Beyond $N_b > 10$, the rate of decline slows down. Furthermore, the difference in the values of Nu_{av} at $\eta_0 = 0$ and 1 increases sharply with increasing N_b for $N_b \leqslant 20$. This also corresponds to the range of interest in most practical applications. Higher values of N_b are obtained for high values of δ/d_p (> 7) [4, 5] leading to low heat transfer rates. Moreover, as discussed by the authors [5], an increase in δ/d_p causes a simultaneous increase in N_b and a decrease in η_0. This is expected to compound the adverse effect of increasing δ on Nu_{av}.

The results presented in this paper are for a constant bed porosity. However, as reported by several authors [8, 17–19] the porosity in the vicinity of the contact surface for flowing granular beds is a function of bed depth and flow velocity of solids. As suggested by Spelt *et al.* [8] (and verified visually in this study), the bed porosity (ε) increases with increasing N and decreasing bed hold-up. This affects h_{av} adversely. It has been illustrated that for a bed of spherical glass beads a 100% increase in ε diminishes Nu_{av} by about 60% [4]. Therefore, assuming ε to be constant over a wide range of agitator speeds (e.g. $N = 5$–100 rev min^{-1}) may introduce significant errors in the estimation of h_{av}.

The results presented above were simulated assuming a particle surface roughness of $s_r = 10$ μm (common value for most materials). Schlunder [19] suggests using $s_r = 0$ (perfectly smooth surfaces) to estimate h. A decrease in s_r overestimates h. This is assumed to compensate for the fact that a particle contacting the surface is slightly deformed and thereby increases its contact surface area. The model for estimating h [15, 19] assumes a point contact. However, it was found in this study that assuming $s_r = 0$ greatly overestimates h_{av} values as compared to experimentally measured ones.

The effect of s_r on Nu_{av} for a bed of rice particles is shown in Fig. 5. Nu_{av} for $s_r = 0$ is about 35% higher as compared to that for $s_r = 10$ μm at $N = 5$ rev min^{-1}. For $N = 100$ rev min^{-1} this difference more than doubles in magnitude. Beyond $s_r = 10$ μm the rate of decrease of Nu_{av} gradually slows down.

The average surface roughness for all model particles (except glass beads) was measured under a binocular vision microscope to be between 15 and 25 μm. Therefore, in all simulations (for verifying experimental results) s_r was assumed to be approximately half of the average particle roughness, i.e. 12 μm for rice, and 7 μm for linseed and millet particles. This reduction in s_r is expected to compensate for the increase in particle–surface contact area due to particle deformation [19] and lead to satisfactory results. For glass beads s_r was taken from the literature [20,

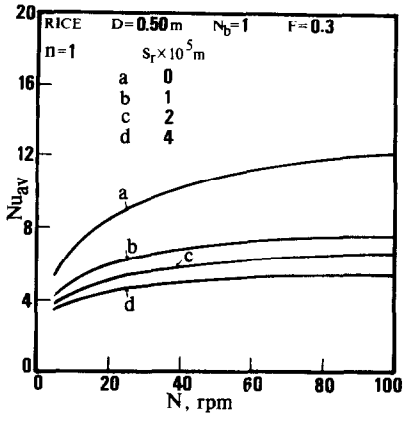

FIG. 5. Effect of particle surface roughness on Nu_{av}.

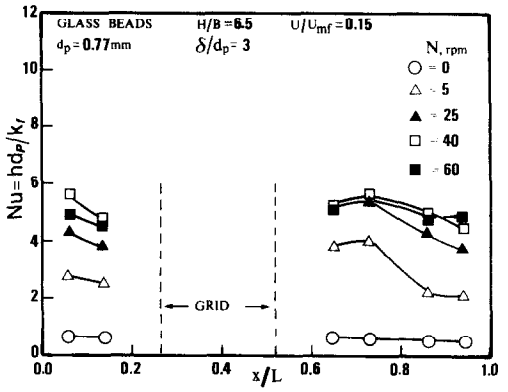

FIG. 7. Effect of agitator speed on Nu.

21]. However, the exact knowledge of s_r and particle deformation is yet elusive and is one of the major limitations of using Schlunder's model [4, 15, 19] for estimating h, as it can introduce significant uncertainties in the predictions.

The effect of δ/d_p ratios on Nu_{av} for beds of free-flowing millet ($C = 0.08$) and rice ($C = 0.12$) is presented in Fig. 6. It shows that for both particles, increasing δ/d_p ratio adversely affects Nu_{av}. However, the reduction in Nu_{av} is more severe for free-flowing particulate beds. Whereas a five-fold increase in δ/d_p from 2 to 10 at $N = 25$ rev min^{-1} decreases Nu_{av} for beds of rice by about 13%, the corresponding drop for beds of millet is more than 40%. The adverse effect of δ/d_p on Nu_{av} diminishes with increasing N. It can therefore be inferred that for granular beds of lower flowability ($C \geqslant 0.11$) stirred by paddle-type blades, increasing δ would have a minimal effect on the contact heat transfer rates (for $\delta/d_p \leqslant 10$).

Experimental results

Figure 7 displays the variation of the measured local Nusselt number (Nu) as a function of the agitator speed. The abscissa denotes the location of the thermocouple employed to record the wall temperature. L includes the circumferential length of the grid and the heated surface. Figure 7 shows that the heat transfer rates are higher over the heated section immediately after the grid (i.e. $x/L > 0.562$). This also corresponds to the region of high particle displacements, i.e. when the number of blade passes required by a particle to traverse the length from $x/L = 0.562$ to 1 is about 3 for $\delta/d_p \leqslant 7$ [5] over the entire range of operating parameters. Particle renewal efficiency, η_0, in this zone is greater than 0.3 even for spherical free-flowing particles (for $\delta/d_p < 8$). Furthermore, all particles contacting the heated surface immediately beyond the grid ($x/L > 0.562$) are freshly renewed from within the bulk or from above the air distributor. This leads to high rates of heat transfer (equations (5) and (6)).

Note that the computed high values of Nu beyond $x/L = 0.562$ may be partly due to the choice of the bed temperature, T_b. As discussed earlier, the average bed temperature for the heated wall H3 (Fig. 1) was the average bed temperature 2–3 cm above the blade b1. However, particles exposed to the cooler inlet air over the grid may attain lower than the measured bed temperature. This would lead to a reduction in the calculated heat transfer coefficients (as compared to those shown in Fig. 7) due to increased ΔT.

Figure 7 also shows that the heat transfer rates are approximately of the same magnitude for the heated sections H2 and H4. Lower heat transfer rates (as compared to those for H3) are observed for the vertical heated surface H4, due to particle slippage and the observed short circuiting of 'heated particles' in that zone.

Figure 7 also shows that agitation improves Nu_{av} considerably up to $N = 40$ rev min^{-1}. The maximum enhancement in Nu_{av} (>350%) is achieved as N increases from 0 to 5 rev min^{-1}. A further eight-fold increase in N from 5 to 40 rev min^{-1} effects only about a 75% improvement in heat transfer. In fact, at higher values of N ($N = 60$ rev min^{-1}) a reduction in the contact heat transfer rate is observed. As mentioned earlier, this may be attributed to an increase in

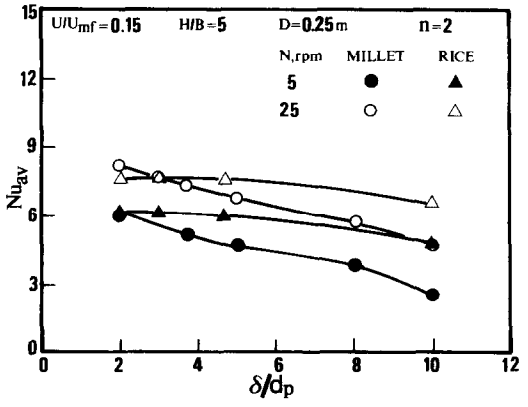

FIG. 6. Effect of δ/d_p and C on Nu_{av}.

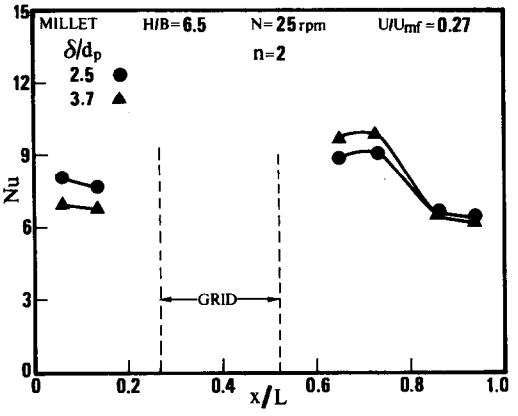

FIG. 8. Effect of δ/d_p on Nu.

the bed porosity along the heated wall which adversely affects the heat transfer rates. This is discussed later on.

Figure 8 displays the effect of δ/d_p on Nu. Increased δ/d_p ratios lead to lower values of Nu except over the region H3 where the opposite trend is observed for free-flowing particles. A possible explanation for this observation was discussed before. With increasing δ/d_p ratios particles stay longer over the distributor grid [4–6] and probably attain thermal equilibrium with the cooler inlet air. This would lead to lower particle temperatures for higher δ/d_p ratios (and hence higher values of ΔT). Particles with $C \geqslant 0.11$ spend very little time over the grid and probably cool down to a lesser extent as compared to free-flowing spherical particles. In accord with this explanation the phenomenon of increasing Nu with increased δ/d_p along the surface H3 was not observed for beds of rice and linseed ($C \geqslant 0.11$).

Figure 9 presents the effect of N on h_{av} for a bed of millet particles. The predicted results were evaluated using equations (5) and (6) and the procedure outlined in ref. [5]. A constant heat flux type boundary condition and a constant bed porosity was employed to estimate h_{av}.

An increase in the δ/d_p ratio causes h_{av} to decrease. This conclusion can be drawn from both the predicted and experimental results in Fig. 9. The effect of air

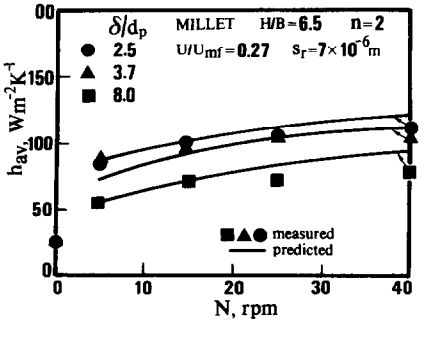

FIG. 9. Effect of δ/d_p on Nu_{av}.

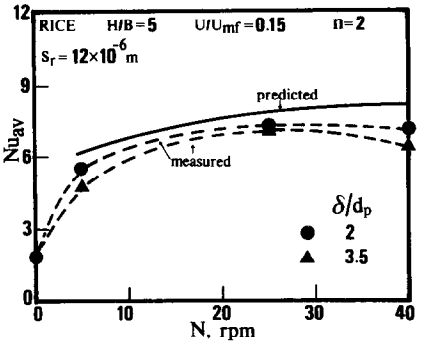

FIG. 10. Effect of δ/d_p on Nu_{av}.

flow rate is incorporated in the model [5] through an increase in the effective bed thermal conductivity. In view of the $\pm 11\%$ experimental uncertainty level in measured values of h_{av} and ± 10 to 15% (combined) for N_b and η_0, the agreement between the experimental and predicted results is fairly good. At higher values of N the heat transfer model overestimates the h_{av} values.

It should be noted that the results in this paper were simulated for a constant bed porosity. Harakas and Beatty [22] reported similar results showing that at higher stirrer speeds the continuum model of heat transfer [23] overestimated h_{av}. This can be attributed to the different thermal responses for gas and solid phases, which implies that for very short contact times (when the thermal wave is not beyond one or two particle diameters), the bed cannot be assumed to behave like a continuum with 'effective' properties. However, in this study, h was evaluated based on a model [15, 19] which included a time independent asymptotic value of thermal contact resistance between the wall and the first layer of contacting particles. For very short contact times, this resistance controls h. As mentioned earlier this resistance is a function of d_p, ε and the interstitial fluid properties. Therefore, any reduction in h with decreasing contact times, i.e. increasing N, may be attributed to an increase in the bed porosity. Since ε increases with increasing N, it is believed that the model deviates at higher values of N due to increasing bed porosity, which was neglected in this study.

For glass beads the deviation between predicted and experimental values of h_{av} was 25–50% at low agitator speeds ($N \leqslant 15$ rev min^{-1}). Increasing the δ/d_p ratio was observed to enhance h_{av}. This is contrary to expectations. The discrepancy is attributed to the unusually high rates of heat transfer recorded for heater H3 with increasing δ/d_p ratio. This leads to poor agreement between predicted and experimental results for $\delta/d_p = 7$. However, for $\delta/d_p = 3$ and $N > 15$ rev min^{-1}, the heat transfer model predicted the experimental results within $\pm 10\%$.

Figure 10 shows a good agreement between predicted and measured values of Nu_{av} for beds of rice. For $N \geqslant 5$ rev min^{-1}, the measured values of Nu_{av}

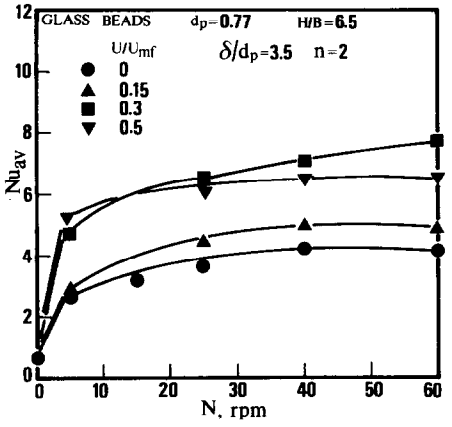

FIG. 11. Effect of aeration on Nu_{av}.

are almost independent of N or decrease slightly. Note that h_{av} is independent of the δ/d_p ratio for beds of rice particles for $\delta/d_p < 3.5$. This is expected, because for beds of rice and linseed particles very little 'particle slippage' was observed for $\delta/d_p < 4$ over the entire range of operating parameters [4, 5] leading to almost constant values for N_b and η_0.

Figure 11 displays the effect of air flow rate on the measured values of Nu_{av} for a bed of glass beads. Increasing air flow rate ($U/U_{mf} \leqslant 0.4$) increases Nu_{av} for $N \leqslant 40$ rev min^{-1}. This effect is attributed to the fact that with increased air flow rate the bed becomes almost thermally well mixed (± 0.3°C variation) and particle renewal occurs at the uniform bed temperature over the entire heated surface. The 'short circuiting' of heated particles is minimal leading to high rates of contact heat transfer.

At low air flow rates ($U/U_{mf} \leqslant 0.2$), the particle renewal at the heated surface probably occurs at higher than the measured bed temperatures. This leads to lower values of heat flux (Q) largely due to 'short circuiting' of heated particles. Since the bed temperature, T_b, was measured at least 20–25d_p from the heated surface, by definition Nu_{av} is lower for low air flow rates ($U/U_{mf} \leqslant 0.2$).

The above arguments also explain the fact that the contact heat transfer model predicts Nu_{av} to a greater degree of accuracy for moderately aerated granular beds as compared to non-aerated or poorly aerated ($U/U_{mf} \leqslant 0.2$) ones. For moderately aerated beds ($U/U_{mf} \geqslant 0.4$) the measured bed temperatures closely represent the actual particle renewal temperatures.

CONCLUSIONS

The key results of the above study may be summarized as follows:

(1) A reduction in the wall-to-blade clearance size and/or an increase in the agitator rotational speed enhances the average contact heat transfer coefficient over the range of parameters examined in this study.

(2) An increase in the δ/d_p ratio adversely affects h_{av} to a greater extent for beds of free-flowing spherical particles ($C \leqslant 0.08$) as compared to the less free-flowing ones ($C \geqslant 0.11$). Increasing agitator speed beyond $N = 25$ rev min^{-1} causes a reduction in h_{av} due to increased bed voidage in the clearance region.

(3) An accurate knowledge of the size of the particle surface asperities and the bed porosity near the contacting surface is important in order to correctly estimate the contact heat transfer coefficient and also rigorously test the physics of the proposed contact heat transfer model.

(4) The presence of aeration (through-air flow) enhances the contact heat transfer rates considerably (up to 50%) over the entire range of operating parameters.

REFERENCES

1. W. L. Root, Indirect drying of solids, *Chem. Engng* May 2, 52–64 (1983).
2. K. Ohashi, Effects of air through-flow on performance of indirect-heat agitated dryer, *Proc. 3rd Int. Drying Symp.*, pp. 467–473 (1982).
3. P. Y. McCormick, The key to drying solids, *Chem. Engng* Aug. 15, 113–122 (1988).
4. K. Malhotra, Particle flow and contact heat transfer characteristics of stirred granular beds, Ph.D. Thesis, McGill University, Montreal, Canada (1989).
5. K. Malhotra and A. S. Mujumdar, Model for contact heat transfer in mechanically stirred granular beds, *Int. J. Heat Mass Transfer* **34**, 415–425 (1991).
6. K. Malhotra, M. Miyahara and A. S. Mujumdar, Estimation of particle renewal rates along the wall in a mechanically stirred granular bed, *Chem. Engng Process.* **27**(3), 121–130 (1990).
7. M. Colakyan and O. Levenspiel, Heat transfer between moving bed of solids and immersed cylinders, *A.I.Ch.E. Symp. Ser.—Fluidization and Fluid Particle Systems*, Vol. 80(241), pp. 156–168 (1984).
8. J. K. Spelt, C. E. Brennen and R. H. Sabersky, Heat transfer to flowing granular material, *Int. J. Heat Mass Transfer* **25**, 791–796 (1982).
9. J. S. M. Botterill and M. Desai, Limiting factors in gas-fluidized bed heat transfer, *Pow. Technol.* **6**, 231–238 (1972).
10. J. Wunschmann and E. U. Schlunder, Heat transfer from heated plates to stagnant and agitated beds of spherical shaped granules under normal pressure and vacuum, *Proc. 5th Int. Heat Transfer Conf.*, Vol. 5, pp. 49–53 (1974).
11. R. Toei, T. Ohmori, T. Furuta and M. Okazaki, *Heat Transfer Coefficient Between Heating Wall and Agitated Granular Bed, DRYING '85* (Edited by R. Toei and A. S. Mujumdar), pp. 209–214. Hemisphere/Springer, New York (1985).
12. K. Malhotra, A. S. Mujumdar and M. Okazaki, Particle flow patterns in a mechanically stirred two-dimensional cylindrical vessel, *Pow. Technol.* **60**, 179–189 (1990).
13. K. Malhotra and A. S. Mujumdar, Particle mixing and solids flowability in granular beds stirred by paddle-type blades, *Pow. Technol.* **61**, 155–164 (1990).
14. K. Malhotra, H. Imakoma, A. S. Mujumdar and M. Okazaki, Fundamental particle mixing studies in an agitated bed of granular materials in a cylindrical dryer, *Pow. Technol.* **55**, 107–114 (1988).
15. K. Malhotra and A. S. Mujumdar, Effect of particle

shape on the particle–surface thermal contact resistance, *J. Chem. Engng Japan* **23**(4), 509–512 (1990).
16. K. Malhotra and A. S. Mujumdar, Immersed surface heat transfer in vibrated fluidized beds, *I&EC Res.* **26**(10), 1983–1992 (1987).
17. C. S. Campbell and C. E. Brennen, Computer simulation of granular shear flows, *J. Fluid Mech.* **151,** 167–188 (1985).
18. J. S. Patton, C. E. Brennen and R. H. Sabersky, Shear flows of rapidly flowing granular materials, *J. Appl. Mech.* **54,** 801–805 (1984).
19. E. U. Schlunder, *Particle Heat Transfer, Proc. 7th Int. Heat Transfer Conf.* (Edited by U. Grigull, E. Hahne, K. Stephan and J. Straub), pp. 195–211. Hemisphere, New York (1982).
20. P. Lybaert, Contribution à l'étude du transfert de chaleur entre un matériau particulaire et la paroi dans les échangeurs rotatifs indirects, Ph.D. Thesis, Faculté Polytechnique de Mons, Belgium (1984).
21. N. N. Mohsenin, *Physical Properties of Plants and Animal Materials*. Gordon & Breach, New York (1970).
22. N. K. Harakas and K. O. Beatty, Moving bed heat transfer: effect of interstitial gas with fine particles, *Chem. Engng Symp. Ser.* **59**(41), 122–128 (1963).
23. H. S. Mickley and D. F. Fairbanks, Mechanism of heat transfer in fluidized beds, *A.I.Ch.E. Jl* **1,** 374–384 (1955).

FLUX THERMIQUE AU CONTACT PAROI-LIT DANS DES LITS GRANULAIRES BRASSES MECANIQUEMENT

Résumé—On présente des résultats expérimentaux et simulés pour le coefficient de transfert de chaleur au contact paroi-lit dans des lits granulaires brassés par des lames. Les observations expérimentales sont prédites correctement par le modèle de renouvellement particulaire à la paroi. On présente et on discute les effets de la vitesse de l'agitateur, du jeu entre paroi et lame, de la fluidité du lit, du débit d'air, de la rugosité de la particule, sur les flux thermiques au contact.

KONTAKTWÄRMEÜBERTRAGUNG VON EINER WAND AN EINE MECHANISCH BEWEGTE SCHÜTTUNG

Zusammenfassung—In dieser Arbeit wird über experimentelle und berechnete Ergebnisse für den Kontakt-Wärmeübergangskoeffizienten von einer Wand an eine mit Schaufeln mechanisch bewegte Schüttung berichtet. Die Beobachtungen im Versuch bestätigen das "Erneuerungs"-Modell bei der Kontaktwärmeübertragung. Folgende Einflüsse auf den Wärmeübergang werden vorgestellt und diskutiert: Rührgeschwindigkeit, Abstand zwischen Wand und Rührschaufeln, Fließfähigkeit der Feststoffpartikel, Strömungsgeschwindigkeit der Luft und Rauhigkeit der Oberfläche.

СКОРОСТИ ТЕПЛОПЕРЕНОСА ПРИ КОНТАКТЕ СТЕНКИ И СЛОЯ В МЕХАНИЧЕСКИ ПЕРЕМЕШИВАЕМЫХ ГРАНУЛИРОВАННЫХ СЛОЯХ

Аннотация—Представлены экспериментальные данные и результаты моделирования коэффициента контактного теплопереноса между стенкой и слоем гранулированного материала, перемешиваемого лопаточными мешалками. Показано, что экспериментальные данные достаточно хорошо предсказываются моделью смены частиц при контактном теплопереносе. Описывается и обсуждается влияние скорости вращения мешалки, зазора между стенкой и лопастями, текучести твердых тел, расхода воздуха и шероховатости поверхности частиц на скорость контактного теплопереноса.